Supporting information

Nano-spatially confined Pd-Cu bimetals in porous N-doped carbon as electrocatalyst for selective denitrification

Tianhang Gu,[a] Wei Teng,[a] Nan Bai,[a] Zehan Chen,[a] Jianwei Fan,[a] Wei-xian Zhang[a] and Dongyuan Zhao[b]*

[a]State Key Laboratory for Pollution Control, School of Environmental Science and Engineering, Shanghai Institute of Pollution Control and Ecological Security, Tongji University, Shanghai 200092, P. R. China

[b]Department of Chemistry, State Key Laboratory of Molecular Engineering of Polymers, Shanghai Key Lab of Molecular Catalysis and Innovative Materials, Laboratory of Advanced Materials, iChEM, Fudan University, Shanghai 200092, P. R. China

Experimental

Preparation of Cu-BTC

The Cu-BTC was prepared by the same method as the PVP/Cu-BTC except without addition of PVP.

Preparation of Pd-Cu/C

The Pd-Cu/C was prepared with the same procedures of Pd-Cu/PNC, except the activated Cu-BTC instead of PVP/Cu-BTC powder.

Preparation of Pd/Cu bulk

The Pd-Cu/PNC-5%-400 was calcinated in muffle furnace to remove the carbon, and then treated in N_2 at 400°C for 4 h again to obtain Pd-Cu bulk.

Characterization

Porosity of the material was determined by N_2 adsorption at 77 K by a Micromeritics Tristar 2420 analyzer. All the samples were previously dehydrated at 423 K for 6 h. The surface area was calculated from the adsorption data at a relative pressure range of 0.02 – 0.2 using the Brunauer-Emmett-Teller (BET) equation. Pore size distribution was calculated by using the Barrett-Joyner-Halenda (BJH) model. The leaching metal amount in the solution was analyzed by inductive coupled plasma-atomic emission spectrometer (ICP-AES) using an Agilent 720ES. Thermogravimetric (TG) analysis was carried out on a Discovery Thermal Gravity Analysis (TGA) at nitrogen stream with 10 K/min.

Analytical methods

The concentration of nitrate, nitrite and ammonium was determined by UV-Vis spectrophotometer (DR-6000, Hach Co., USA) according to standard methods. Detailed procedures were based on previous report.[1, 2]

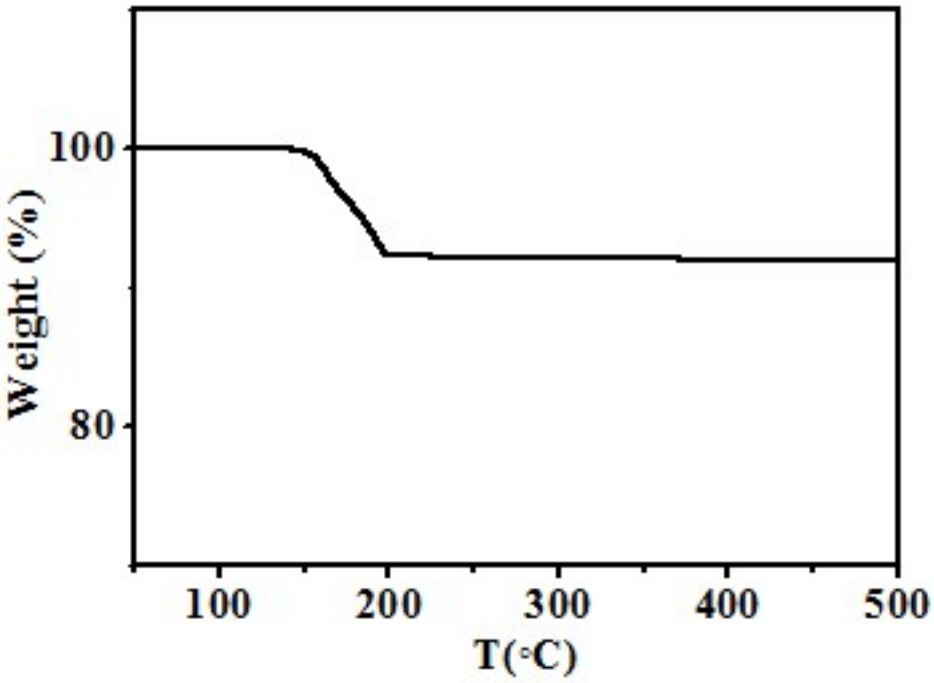

Fig. S1 The TGA curve of $Pd(acac)_2$ under N_2 atmosphere. $Pd(acac)_2$ can be decomposed above 200°C.

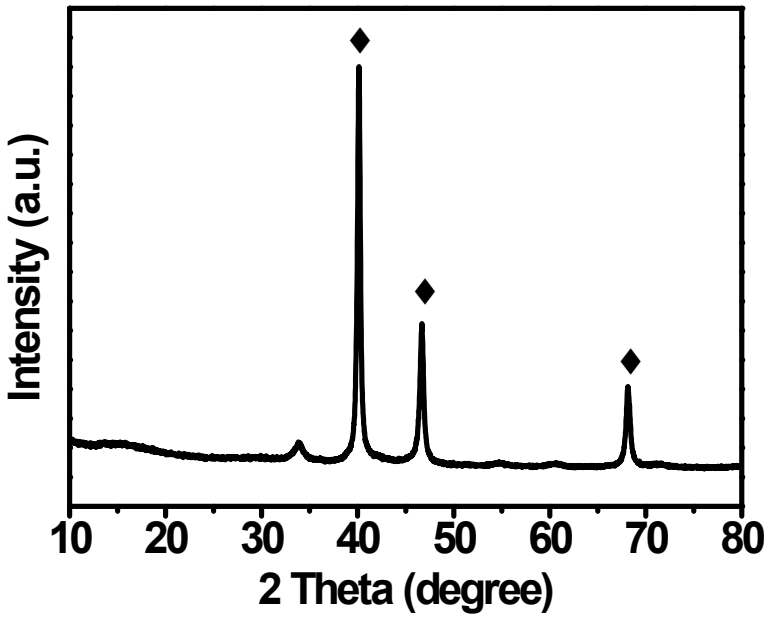

Fig. S2 The XRD pattern of $Pd(acac)_2$ after pyrolysis under nitrogen atmosphere at 250°C, showing the formation of metallic Pd(0).

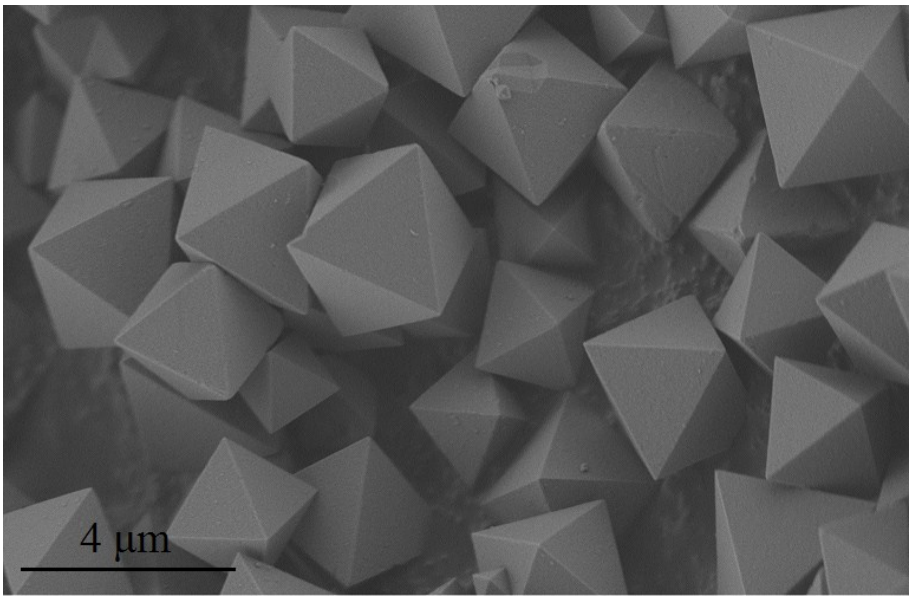

Fig. S3 The SEM image of PVP/Cu-BTC（3 g of PVP addition with hydrothermal treatment for 12 h at 393 K）. After pyrolysis, the size of the single crystal decreases from 2-4 to 1-2 μm due to the contraction of frameworks.

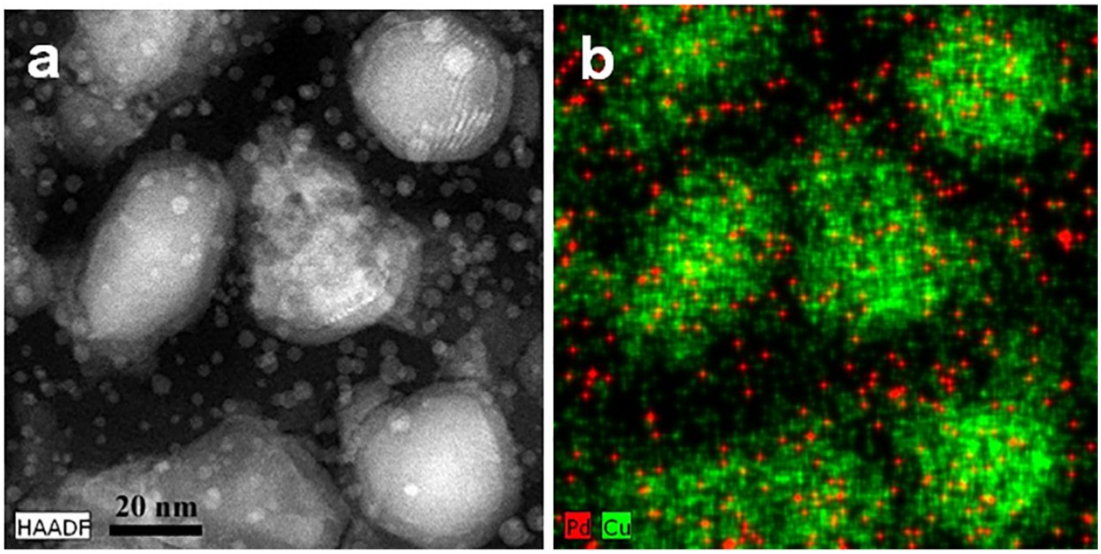

Fig. S4 a) High-angle annular dark-field (HAADF) scanning transmission electron microscopy (STEM) image and b) energy dispersive spectrometer (EDS) elemental mappings of ultrathin slice of Pd-Cu/PNC (Pd-Cu/PNC-5%-400 with 5% of $Pd(acac)_2$ and pyrolysis at 400°C, and green represents Cu and red is Pd).

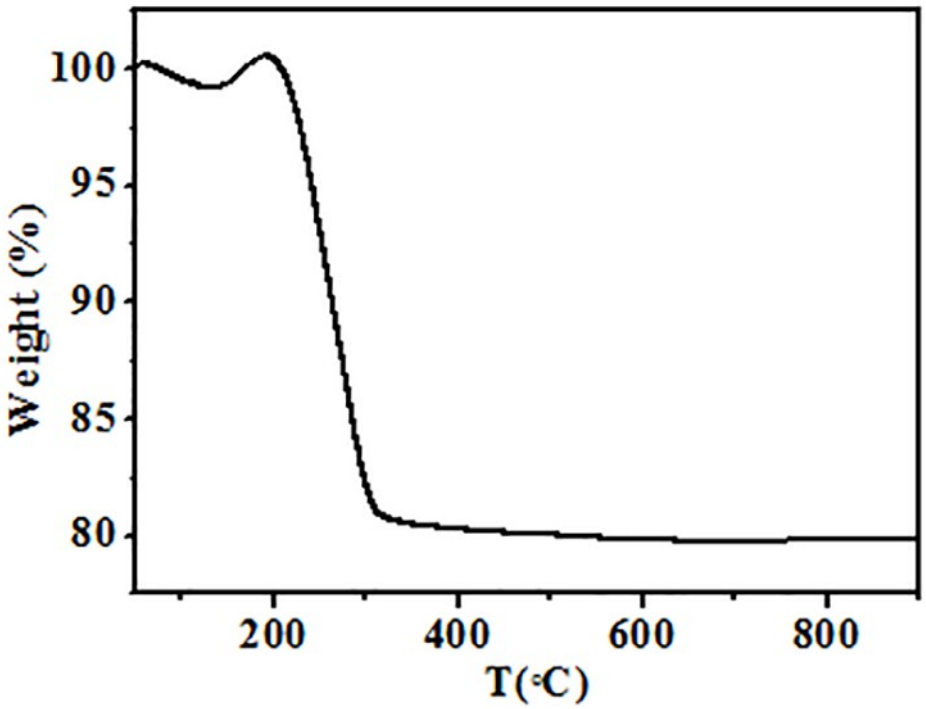

Fig. S5 The TGA curve of Pd-Cu/PNC under O_2. Rising weight at about 200°C suggested the oxidation of the metals. About 20 wt. % mass loss at 900°C implied that the oxides of Cu and Pd account for 80 wt. %, identified with the ICP results that 55 wt. % of Cu and 10 wt. % of Pd.

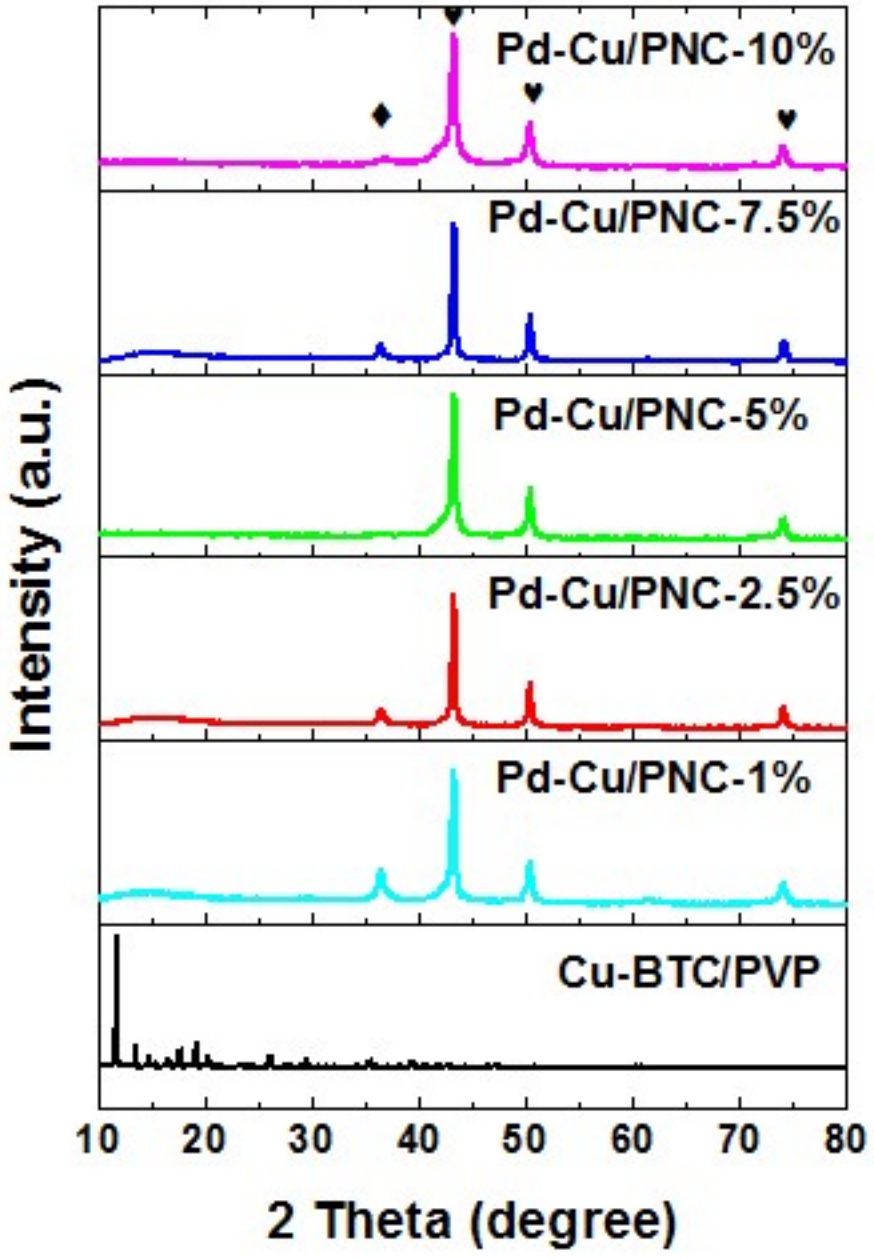

Fig. S6 XRD patterns of PVP/Cu-BTC without calcination and Pd-Cu/PNC series with different Pd addition.

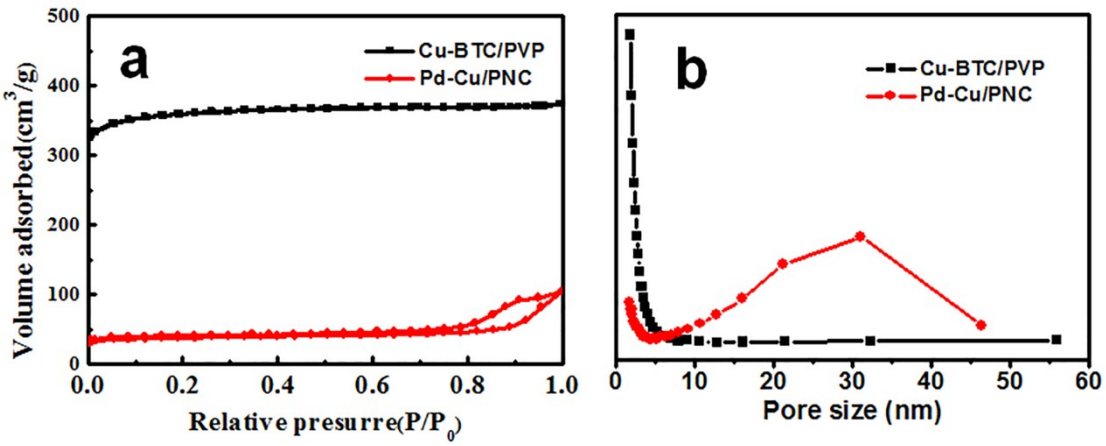

Fig. S7 a) Nitrogen sorption isotherms and b) corresponding pore size distributions of Pd-Cu/PNC (Pd-Cu/PNC-5%-400 with 5% of $Pd(acac)_2$ and pyrolysis at 400°C) and pristine PVP/Cu-BTC without pyrolysis.

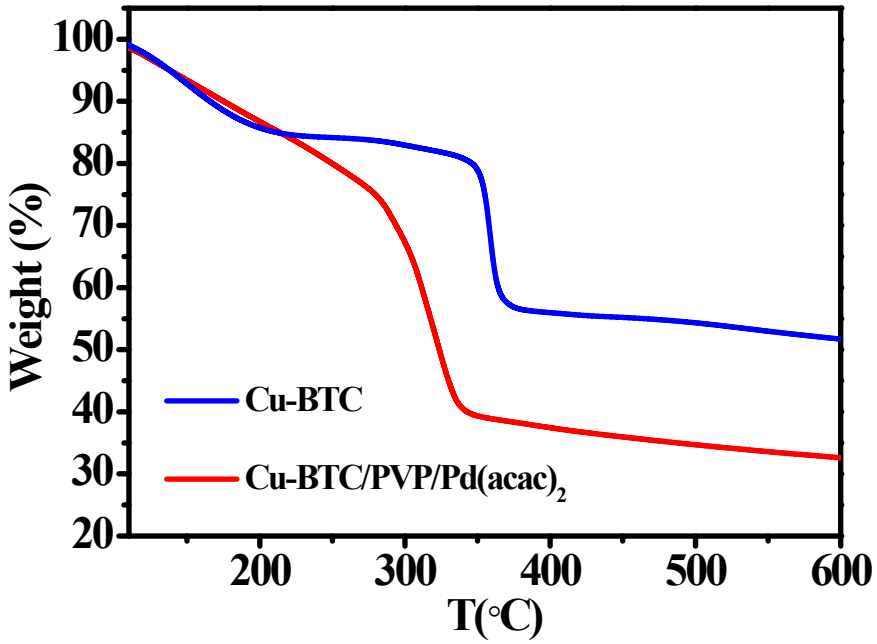

Fig. S8 TGA curves of Cu-BTC and PVP/Cu-BTC/$Pd(acac)_2$ under N_2 atmosphere.

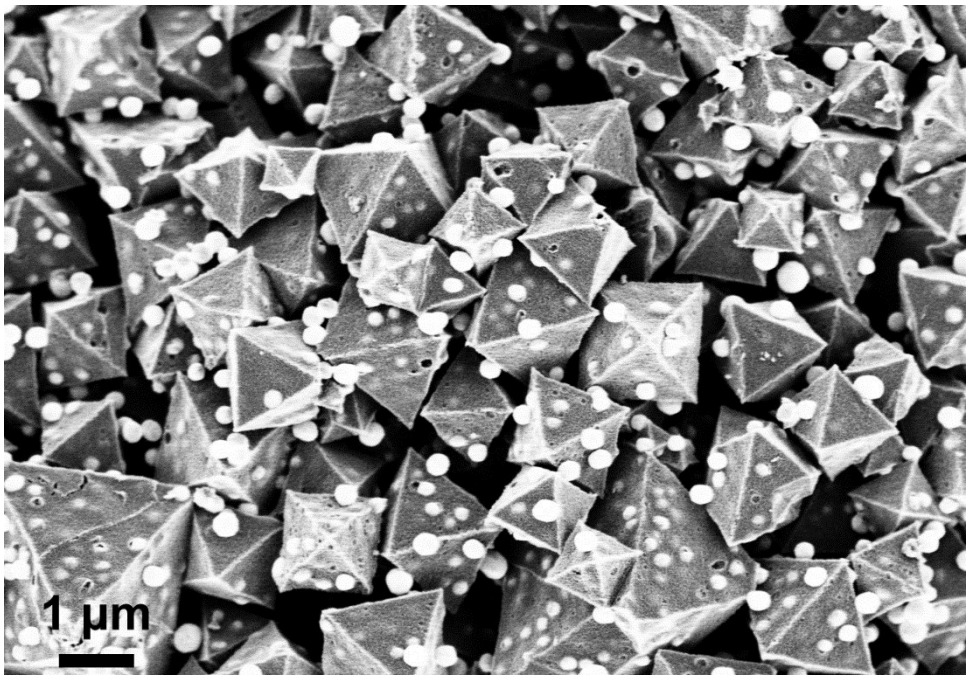

Fig. S9 The SEM image of Pd-Cu/PNC-5%-700 treated at 700°C.

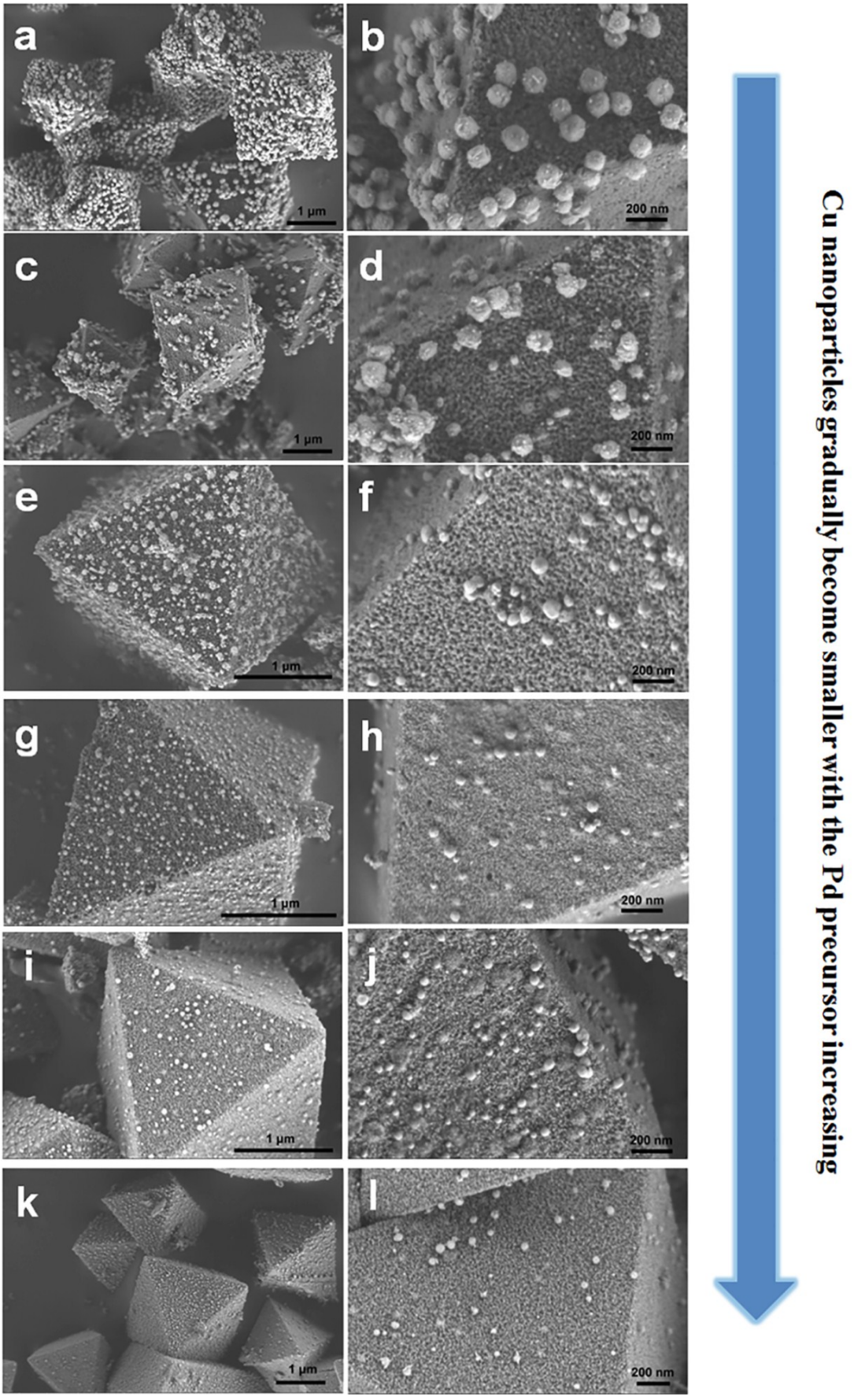

Fig. S10 SEM images of Pd-Cu/PNCs with different $Pd(acac)_2$ additions

with (a, b) 0.25%, (c, d) 1%, (e, f) 2.5%, (g, h) 5%, (i, j) 7.5% and (k, l) 10%.

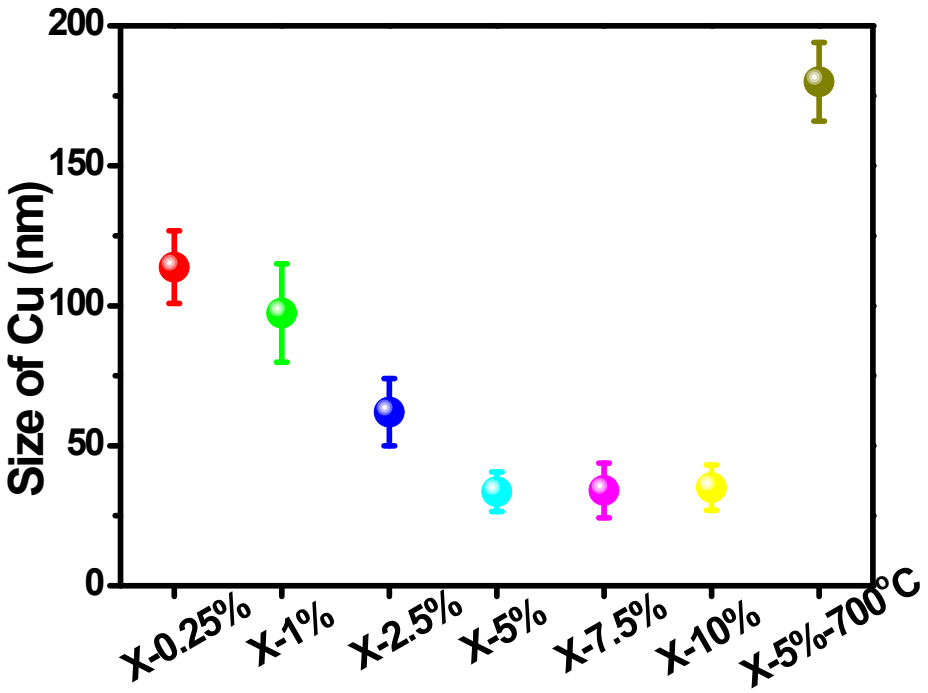

Fig. S11 The evolution of Cu sizes in Pd-Cu/PNC series with increased $Pd(acac)_2$ additions and calcination temperatures based on SEM results (X = Pd-Cu/PNC).

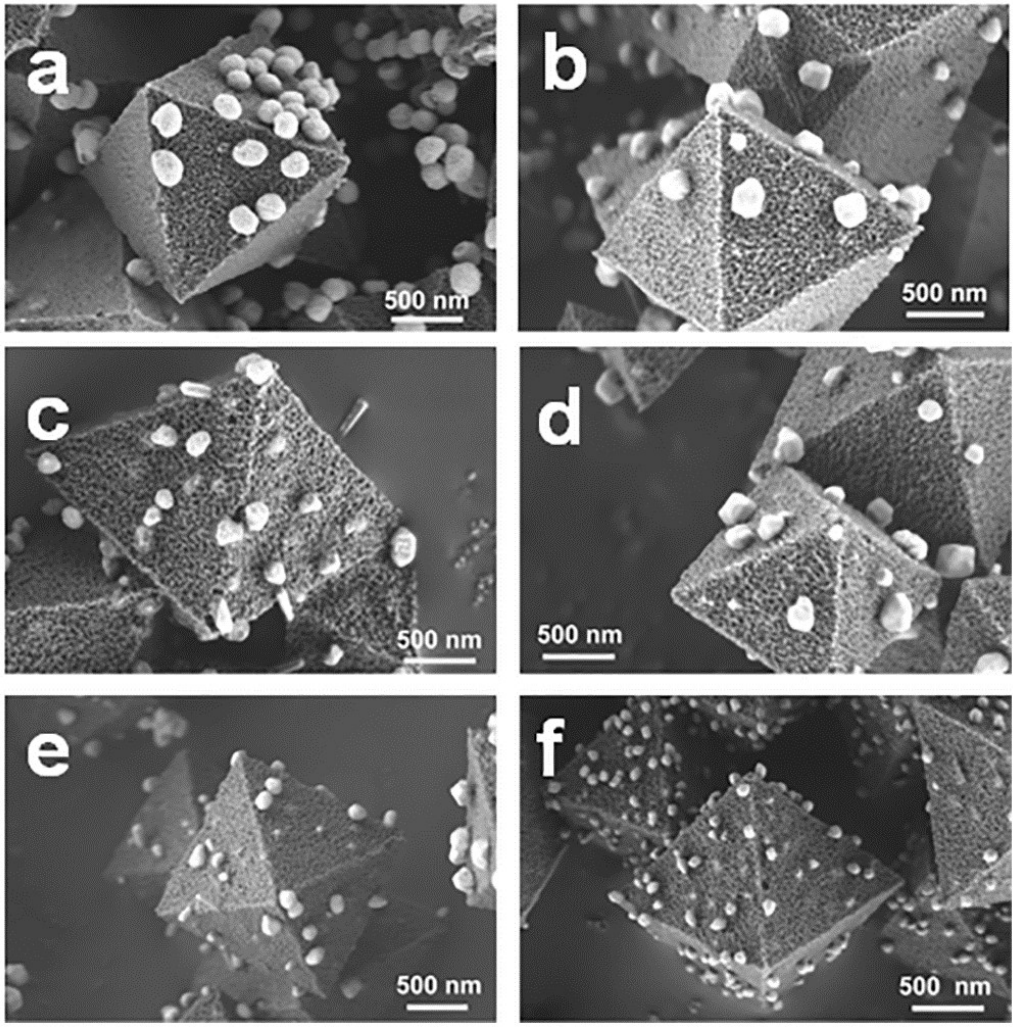

Fig. S12 SEM images of Cu/PNC without Pd(II) but only addition of acetylacetone which were equivalent to that in the $Pd(acac)_2$ of Pd-Cu/PNC with a) 0, b) 1, c) 5, d) 7.5, e) 10, and f) 15%, respectively.

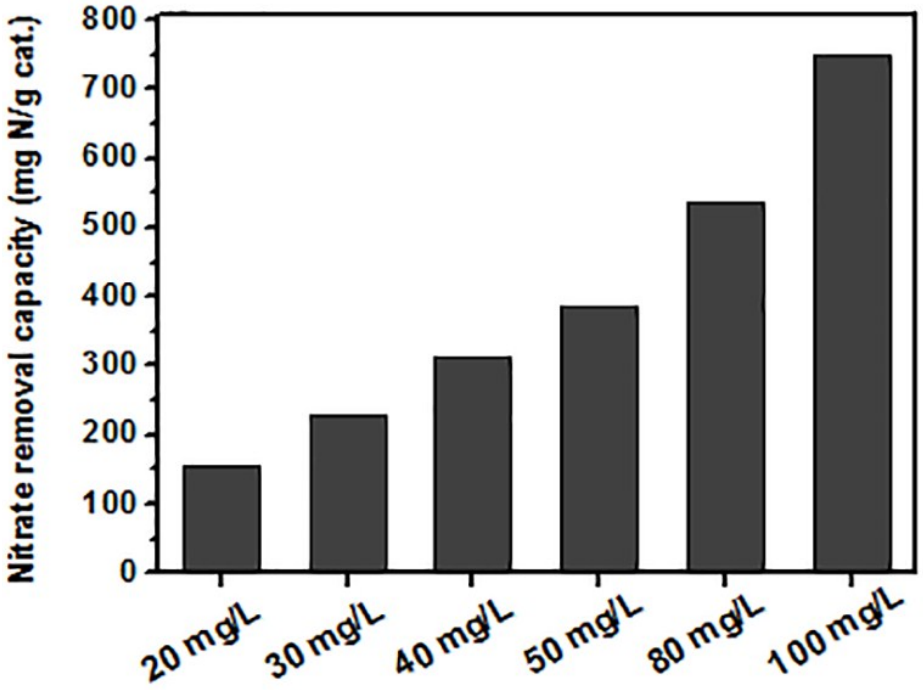

Fig. S13 Nitrate removal capacity on Pd-Cu/PNC (Pd-Cu/PNC-5%-400 with 5% of $Pd(acac)_2$ and pyrolysis at 400°C) for denitrification at different initial concentration of nitrate (0.1 M Na_2SO_4, -1.3 V *vs*. SCE and 24 h).

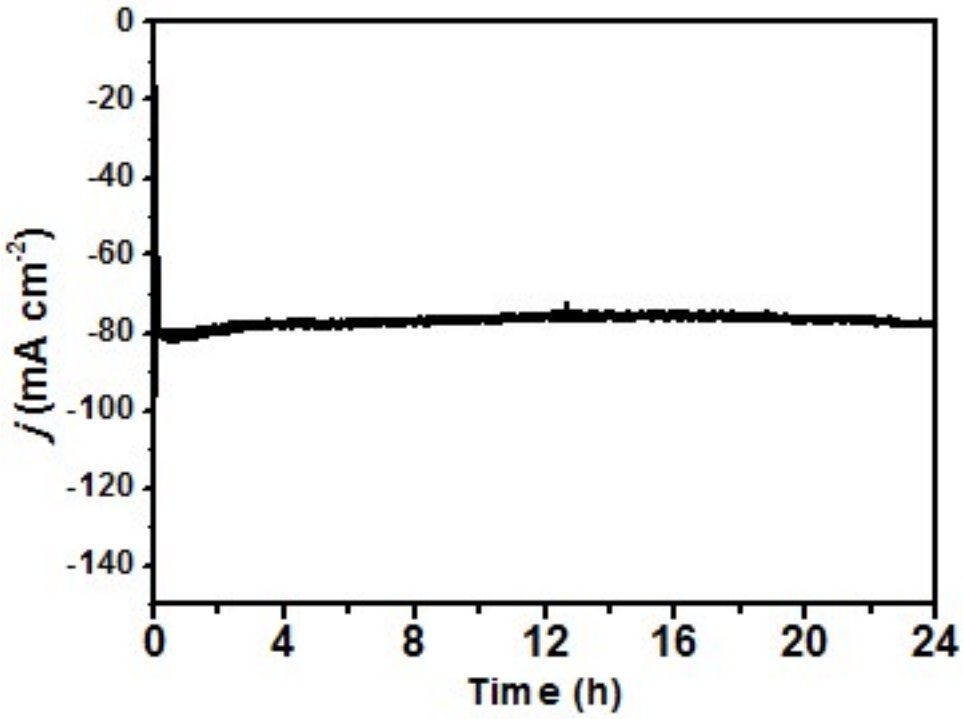

Fig. 14 Current density for 24 h of electrolysis at -1.3 V *vs*. SCE with Pd-Cu/PNC-5%-400 on a nickel foam plate (4 × 4 cm) in the presence of 1 L 100 mg N/L nitrate and 0.1 M Na_2SO_4.

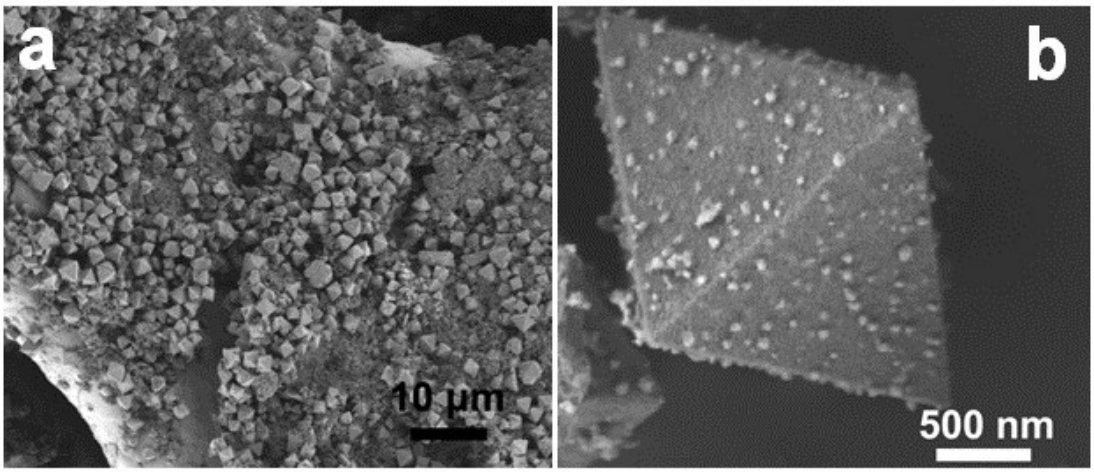

Fig. S15 SEM images of Pd-Cu/PNC (Pd-Cu/PNC-5%-400 with 5% of $Pd(acac)_2$ and pyrolysis at 400°C) after eight cycles of denitrification.

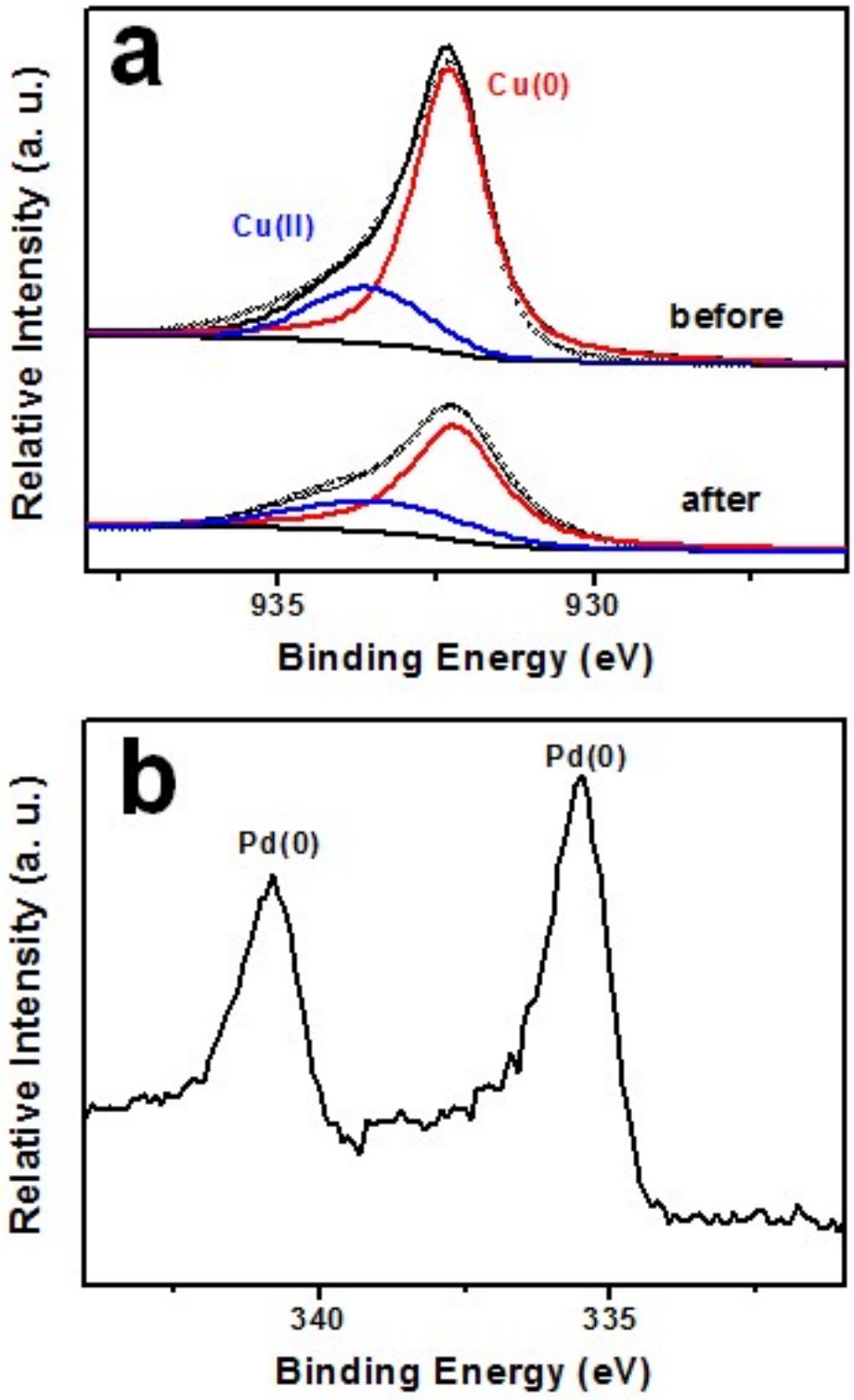

Fig. S16 High-resolution a) Cu 2p and b) Pd 3d XPS spectra of Pd-Cu/PNC (Pd-Cu/PNC-5%-400 with 5% of $Pd(acac)_2$ and pyrolysis at 400°C) after eight cycles of denitrification.

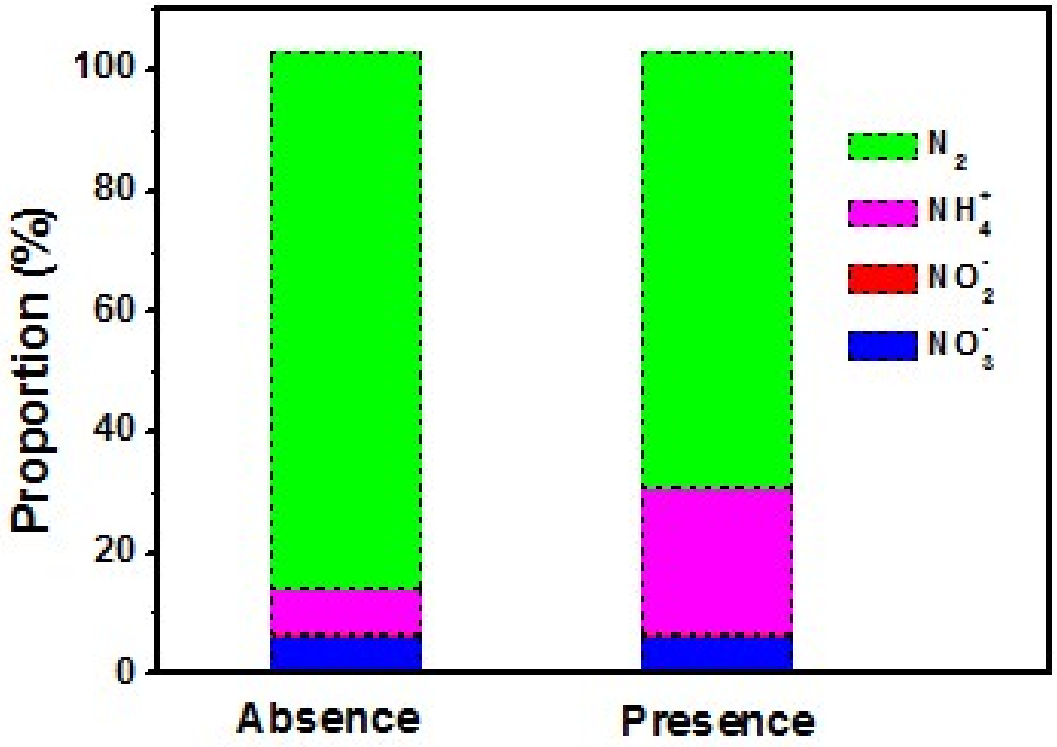

Fig. S17 Proportion of products in the presence and absence of isopropanol after 24 h of electrocatalytic reduction of nitrate at -1.3 V *vs*. SCE on Pd-Cu/PNC (Pd-Cu/PNC-5%-400 with 5% of $Pd(acac)_2$ and pyrolysis at 400°C, 100 mg N/L of nitrate, 0.1 M Na_2SO_4).

Discussion: Isopropanol scavenger was added into the initial solution. The concentration of final nitrate and nitrite was nearly the same compared with that without isopropanol addition, but more ammonium was detected (7.6 to 24%). Because the isopropanol was used to scavenge HO • , it could be inferred that the HO • generated at the anode and might oxidize ammonium to dinitrogen to a certain extent.

Table S1. The contents of components in Cu/PNC and Pd-Cu/PNCs with different $Pd(acac)_2$ addition.

Sample	ICP		Elemental analysis	Weight ratio of Cu and Pd
	Cu (%)	Pd (%)	N (wt. %)	
Cu/PNC	63	0	1.8	-
Pd-Cu/PNC-0.25%	58	0.45	-	130:1
Pd-Cu/PNC-1%	53	1.9	-	28:1
Pd-Cu/PNC-2.5%	57	4.8	2.2	12:1
Pd-Cu/PNC-5%	55	10	1.9	5.5:1
Pd-Cu/PNC-7.5%	54	12.5	-	4.3:1
Pd-	51	17	-	3:1

Cu/PNC-

10%

Table S2. Textural parameters of PVP/Cu-BTC and Pd-Cu/PNC (Pd-Cu/PNC-5%-400 with 5% of $Pd(acac)_2$ and pyrolysis at 400°C).

Sample	S_{BET} (m^2/g)	V_t (cm^3/g)	Pore size (nm)
Cu-BTC/PVP	1440	0.56	< 2 nm
Pd-Cu/PNC	154	0.25	< 2 and 30 nm

Table S3. Comparison of electrocatalytic denitrification performance of Pd-Cu/PNC with other materials reported in relevant literature.

Cathode	**Nitrate concentration (mg/L)**	**Electrolyte (M)**	**Potential (V)**	$X_{NO_3^-}$ **(%)**	S_{N_2} **(%)**	**Energy consumption (kWh mol^{-1})**	**Ref.**
Cu-Bi	100	Na_2SO_4 (0.1)	NM*	87.5	60.8	NM*	[3]
Magnéli phase REMs	14	$NaHCO_3$ (0.1)	-2.5	67	56	2.4	[4]
Cu-Ni	620	NaOH (0.01)+ NaCl (0.5)	-1.3	91.9	NM*	1.43	[5]
Sn-Pd	140	$HClO_4$ (0.1)	-0.2	41	51.3	NM*	[6]
Pd-Cu/graphite	85000	NaOH (1)	-1.1	NM*	70	NM*	[7]
Cu-Ni alloy	28	NaCl or Na_2SO_4 (2.5 mM)	-1.8	70	NM*	NM*	[8]
Pd-Cu/PN-C	100	Na_2SO_4 (0.1)	-1.3	97	83	0.75	Our work

NM* means not mentioned in the literature.

References

1 A. E. Palomares, J. G. Prato, F. Márquez and A. Corma, *Appl. Catal. B- Environ.,* 2003, **41**, 3-13.

2 W. Teng, N. Bai, Y. Liu, Y. Liu, J. Fan and W. Zhang, *Environ. Sci. Technol.*, 2018, **52**, 230-236.

3 W. Gao, L. Gao, D. Li, K. Huang, L. Cui, J. Meng and J. Liang, *J. Electroanal. Chem.*, 2018, **817**, 202-209.

4 P. Gayen, J. Spataro, S. Avasarala, A. Ali, J. M. Cerrato and B. P. Chaplin, *Environ. Sci. Technol.*, 2018, **52**, 9370-9379.

5 D. Reyter, D. Bélanger and L. Roué, *J. Hazard. Mater.*, 2011, **192**, 507-513.

6 M. Motahar Hossain, K. Nakata, T. Kawaguchi and K. Shimazu, *J. Electroanal. Chem.*, 2013, **707**, 59-65.

7 O. Ghodbane, M. Sarrazin, L. Roué and D. Bélanger, *J. Electrochem. Soc.*, 2008, **155**, F117-F123.

8 J. Ding, W. Li, Q. Zhao, K. Wang, Z. Zheng and Y. Gao, *Chem. Eng. J.*, 2015, **271**, 252-259.